NTNU
Norwegian University of
Science and Technology

Master's thesis

High Accuracy Optical Power Measurements – Using Silicon Photodetectors as Primary Standards

Måling av Optisk Effekt med Silisium Fotodetektorer som Primærnormal

Guro Flatøy

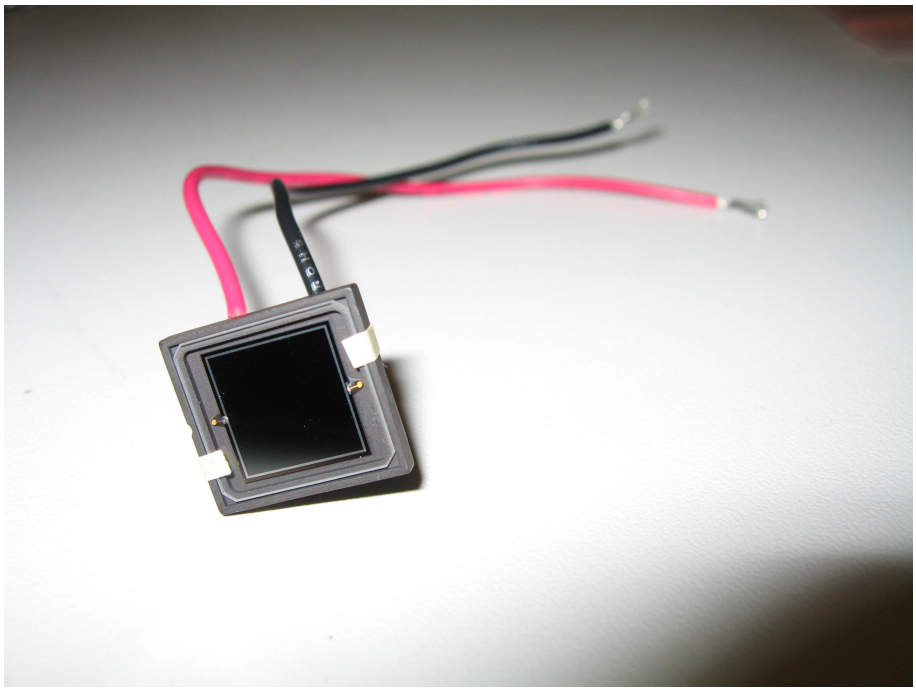

June 15, 2009

Abstract

To use silicon photodetectors as primary standards, the responsivity of the detector has to be independently determined. For an ideal photodiode the responsivity is given solely by fundamental constants and the wavelength of the incident light. Silicon photodetectors can be modelled as an ideal photodiode including the two major loss components; reflection from the detector surface and recombination losses. With known oxide thickness, refractive indices and angle and polarization of the incident light, the spectrally dependent reflectance can be calculated from Fresnel's equations. Two different methods for determining the recombination losses, known as the internal quantum deficiency, are examined in this master's thesis. One method involves fitting the measured relative response of the silicon detector to an expression of the internal quantum deficiency. It is examined if the relative response of the detector can be determined, with higher accuracy than previously obtained, by using a laser as the light source. The other method is known as the "self-calibration procedure". This determines the internal quantum deficiency by applying a bias voltage over appropriate regions of the detector. It is examined if the self-calibration procedure can be carried out using a detachable gold electrode to apply the oxide bias.

Sammendrag

For å kunne bruke silisium fotodetektorer som primærnormal må responsiviteten til detektoren bestemmes uavhengig av en referansedetektor med kjent responsitivitet. For en ideell fotodiode er responsiviteten gitt utelukkende av naturkonstanter og bølgelengden til det innfallende lyset. Silisium fotodetektorer kan modelleres som en ideell diode hvor man inkluderer de to viktigste tapskildene; refleksjon fra overflaten og rekombinasjonstap. Med kjent oksidtykkelse, brytningsindekser og vinkel og polarisasjon til det innfallende lyset, kan den spektralt avhengige reflektansen beregnes fra Fresnels ligninger. To forskjellige metoder for å bestemme rekombinasjonstapene, også kjent som kvantedefekten, er undersøkt i denne master oppgaven. Den ene metoden går ut på å tilpasse den målte relative responsen til silisium

detektoren til et uttrykk for kvantedefekten. Det er undersøkt om den relative responsen til detektoren kan bestemmes med større nøyaktighet enn i tidligere eksperimenter ved å bruke en laser som lyskilde. Den andre metoden som er undersøkt er kjent som "selvkalibreringsmetoden". Denne bestemmer kvantedefekten ved å sette spenning over ulike regioner av detektoren. Det er undersøkt om selvkalibreringsmetoden kan utføres ved å bruke en avtagbar gullelektrode til å sette spenning over oksidet.

Preface

This master's thesis constitute the 10^{th} semester of the master degree study in technical physics at the Department of Physics at the Norwegian University of Science and Technology (NTNU).

The work has been carried out at the Norwegian Metrology Service (JV) under the supervision of Jarle Gran. Responsible supervisor at NTNU has been Berit Kjeldstad.

I would like to thank my supervisor Jarle Gran for excellent guidance and support both with the experimental work and the writing of this thesis. I would also like to thank the Norwegian Metrology Service for disposing a lab with all the necessary equipment during the entire semester

Contents

Chapter 1

Introduction

Measuring optical radiation is necessary within a number of industries, for instance medicine, telecommunication, lighting, defence and so on. The measurements are used to obtain information about a source that radiates, or about a sample that reflects, absorbs or transmits light. Optical radiation can also be used to transfer information the same way lower wavelength radio waves have been used for decades. Since the invention of the laser, optical radiation measurements has obtained a vast number of new applications. Laser measurements can for instance be used to determine distance, which is used to control dimensions of industrial products and in traffic control to determine the speed of a vehicle. In medicine there is a number of treatments involving radiation in the infrared, visible and ultraviolet region. Light treatment of jaundice in newborn, laser surgery and use of blue light for dental treatment are just a few examples.

New areas where optical radiation measurements are used continuously emerges since these measurements rarely causes harm or damages the object that is radiated. An example of this is the use of absorption measurements to determine fat contents and colour of salmon[1]. Many of these new applications require a high degree of measurement accuracy, as small variations in the measurements can correspond to large variations in the property being investigated.

The ideal detector is accurate, low cost, stable and portable. The detector should also have a uniform response across its active area, a good linearity, short time constant, and a high signal-to-noise ratio. Silicon photodetectors meet these demands[2]. They can easily be used to carry out high accuracy measurements, but first must the electrical output per optical input, the responsivity of the detector, be determined. Determining the responsivity of a silicon detector, without using a reference detector with known responsivity, is at the moment not possible to a high enough degree of accuracy. This is why silicon detectors are not primary standards today.

A primary standard is the standard which is recognized as having the highest degree of accuracy, and which yields a value which can be accepted without refering to other standards of the same unit of measurement[3]. Todays primary standard is the cryogenic radiometer. A cryogenic radiometer is generally an electrical subsitution radiometer, which consists of a blackened metal cavity which is attached to a constant temperatur heat sink[4]. When exposed to radiation the temperature of the cavity will rise. By attaching an electrical heater to the blackened cavity one can heat it to the same temperature as obtained by the radiation. The electrical power used to heat the cavity will be the same as the radiated power. The cryogenic radiometer operates at 4.2 K and in a vacuum, which eliminates many of the corrections needed for the room temperature electrical subsitution radiometers[4] A cryogenic radiometer is a complicated and expensive piece of equipment, which only a few laboratories can afford.

To use silicon detectors as primary standards one has to independently determine the detectors responsivity with a very high degree of accuracy. An attempt at this was done in 1980 when *E. F. Zalewski* and *J. Geist* developed the "self-calibration procedure"[5]. This procedure consists of applying a bias voltage over different parts of the detector, and by doing so lowering the losses in the detector to negligleble levels. By measuring the change in the detector response, one can determine the fraction of light which is not detected at normal operation mode. Because the detectors responsivity is determined without use of a reference detector, the procedure is known as the "self-calibration procedure". This procedure is inexpensive and requires a minimum of equipment. The reason why this has not become standard procedure for determining the responsivity of silicon photodetectors is that it somehow alters the qualities of the detector. This was discovered in the early eighties and the interest of the self-calibration procedure was gradually lost. Another way of determining the responsivity of a silicon photodetector was developed by *J. Gran* and *A. S. Sudbø* in 2003[6]. This procedure involves fitting an expression of the detectors internal losses to the measured relative response of a silicon detector. This method can be used in combination with the self-calibration procedure.

The self-calibration procedure has been investigated in earlier work[7], and in this master's thesis the method is examined further to see if the procedure can be preformed using a detachable gold electrode. If there is some way the degradation of the detector can be avoided or kept at negligible levels, the detachable gold electrode could be used as part of a kit to determine the responsivity of silicon photo detectors. When it comes to the "relative respons procedure" the aim is to investigate whether the already promising results obtained using this method can give even better results by improving the initial measurement set-up by using a laser as the light source.

Chapter 2

Theory

2.1 Basic principles of a photodiode

A photodiode converts received optical power into electrical current. The photodiodes used in this master's thesis are p^+-n silicon diodes. A p-n diode consists of p-type and n-type semiconductor in very close contact. A p-type semiconductor is doped so that it has an excess concentration of holes, while an n-type semiconductor is doped to give an excess concentrations of electrons. A p^+-n diode has a shallower and more heavily doped p-region than n-region.

The junction of the diode is where the p-type and n-type semiconductor meet. At the junction electrons will diffuse from the n-doped side to the p-doped side and recombine with holes on the p-doped side. The same way holes will diffuse from the p-doped side to the n-doped side, and recombine with electrons. This will cause a concentration of positive charge on the n-doped side and negative charge on the p-doped side. The electric field between the p-doped side and the n-doped side will cause a drift current in the opposite direction of the diffusion current. When more charges diffuse across the junction, the electric field gets higher and thus the drift current increases. The electric field will increase until an equilibrium is reached between the drift and diffusion currents[8]. When this equilibrium is reached there is a "built-in" electric field across the junction of the photodiode, see figure 2.1.

Near the junction there will be a region which is positively charged on the n-doped side, and negatively charged on the p-doped side. This region will be almost completely depleted of charge carriers, and is therefore called the depletion region, see figure 2.1.

A photon incident on the photodiode with an energy larger than the band gap of the semiconductor can excite an electron, thus creating an electron-

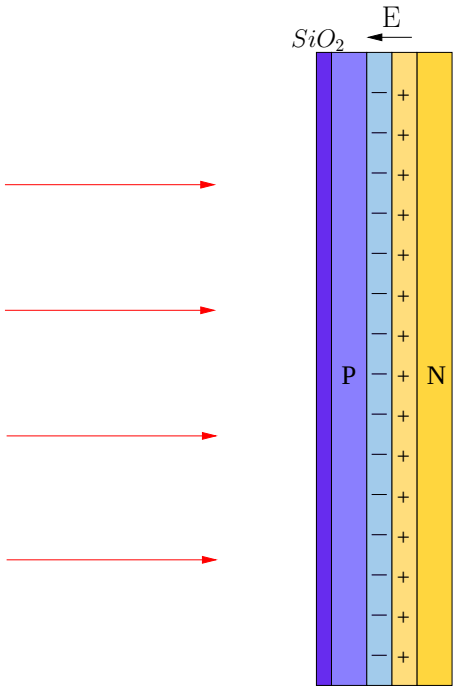

Figure 2.1: Schematic view of a silicon photodetector. To the left is the p-type region covered by the silicon oxide layer. To the right is the n-type region. Between the two regions is the charged depletion region with the "built-in" electric field across the junction. The different regions are not drawn to scale. Red arrows illustrate incident light.

hole pair. If this electron-hole pair is created in the depletion region of the diode, the charge carriers will quickly be swept across the junction by the electric field. Therefore the photodiode can deliver a current depending on the incoming light. If the electron-hole pair is created in the p-doped region of the diode, the electron will have to diffuse to the junction before it can be collected by the electric field. The same way must a hole, created in the n-doped region, diffuse to the junction for collection[8].

During production of the silicon photodetector, a layer of of silicon dioxide is grown on the surface of the diode, see figure 2.1. This layer reflects about 30% of the incident light, which is the most important loss mechanism in silicon photodetectors. This reflection is spectrally dependent. Another loss mechanism is recombination of electron-hole pairs created outside the depletion region. In the depletion region recombination is negligible down to 0,001%[5].

There are three regions in which recombination can occur[9]. The first, and most important, is at the Si-SiO_2 interface, see figure 2.1. Furthermore we

have recombination in the region between the interface and the junction, and in the region to the rear of the junction. Recombination in the different regions will effect different portions of the wavelength spectra, since longer wavelengths penetrate deeper into the device.

The cause of the high recombination probability at the oxide interface is that there is a positive interface charge, Q_i, which repels holes and create a dipole centred at the interface[5]. The dipole electric field increases the concentration of electrons at the interface, and thereby increases their recombination rate through interaction with surface states[5]. The positive interface charge, Q_i, is a combination of charges in the silicon dioxide and charges at the interface. The silicon dioxide charges come from alkali metals incorporated in the oxide during production. These positive ions will be relatively mobile. In addition to this there will also be trapped charges due to imperfections in the oxide[8]. The interface charges is a set of positive charges that results form a sudden termination of the silicon crystal at the oxide interface. During the oxidation process Si is removed from the surface to react with oxygen. Some Si-ions are left at the interface, and together with uncompleted Si-bonds, this results in a sheet of positive fixed charge at the interface[8].

Electron-hole pairs created in the region between the oxide interface and the junction, or in the region to the rear of the junction, must diffuse to the junction before collection[5]. For carriers created to the rear of the junction, the time this takes can be significant with respect to the minority carrier lifetime[5]. For carriers created in the front region recombination losses are negligible compared to the losses caused by surface recombination.

2.2 Silicon photodiodes as primary standards

2.2.1 Modelling silicon photodetectors

The responsivity of a photodiode is the electrical output per optical input. For an ideal photodiode the responsivity is given solely by fundamental constants and the wavelength of the incoming light[6]

$$R(\lambda) = \frac{e\lambda}{hc} \tag{2.1}$$

where R is the responsivity of the photodiode, e is the elementary charge, λ is the vacuum wavelength of the radiation, h is Planck's constant and c is the speed of light in vacuum.

Silicon photodetectors can be modelled as an ideal photodiode including the two major loss components, reflection at the surface and recombination losses. The detector reflectance, $\rho(\lambda)$, yields the fraction of the optical input that is reflected by the silicon oxide surface of the detector[6]. The internal quantum efficiency of a photodetector, $\epsilon(\lambda)$, is the fraction of the transmitted light that gets collected by the "built-in" electric field. The fraction of the optical input lost by recombination is known as the internal quantum deficiency $\delta(\lambda)$, so that $\epsilon(\lambda) = (1-\delta(\lambda))$[6]. Including these loss mechanisms in equation 2.1 one obtains the responsivity of the silicon photodetector

$$R(\lambda) = \frac{e\lambda}{hc}\left(1-\rho(\lambda)\right)\left(1-\delta(\lambda)\right) \tag{2.2}$$

To find the responsivity, the reflectance and the quantum deficiency has to be estimated.

With known refractive indices, silicon oxide thickness, polarization and angle of the incident light, the reflectance can be calculated from Fresnel's equations[6]. Determining the internal quantum deficiency can be done in several different ways. The two ways examined in this thesis is the self-calibration procedure developed by *E. F. Zalewski* and *J. Geist* and the relative response procedure developed by *J. Gran* and *A. S. Sudbø*, which involves fitting an expression of the internal quantum deficiency to the measured relative response of a silicon detector[6].

2.2.2 The relative response procedure

Modelling the internal quantum deficiency

The method for determining the quantum deficiency from purely relative measurements was developed by *J. Gran* and *A. S. Sudbø* [6], and is based on the model of the internal quantum efficiency developed by *Gentile et al* [10]. The model of the quantum deficiency used in this procedure is one minus the model by *Gentile et al.*

The basis of this procedure is a simple model of the recombination probability of the electron-hole pairs, where the recombination probability depends only on the depth where the electron-hole pair is generated[6], see figure 2.2.

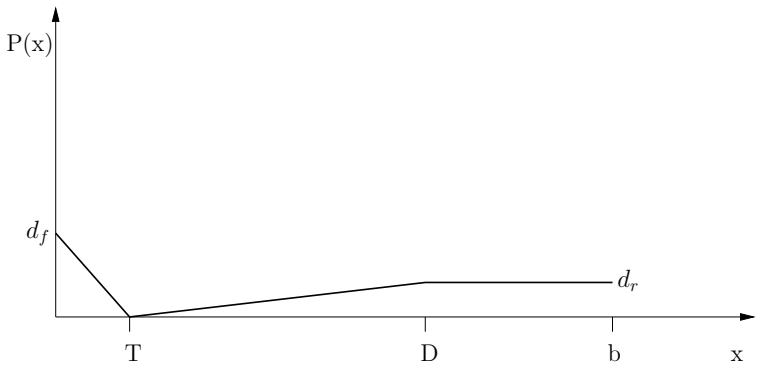

Figure 2.2: Recombination probability P as a function of depth in the detector. d_f is the recombination probability of electron-hole pairs generated at the SiO_2/Si interface. It decreases linearly to zero at T, which is the position of the pn-junction. From T there is a linear increase until D, which is the start of the bulk region of the detector. In the bulk region the recombination probability is d_r. b is the depth of the detector.

The quantum deficiency is found by integrating the recombination probability and the normalized distribution of photons over the depth of the detector[6].

$$\delta = \int_0^b \mathrm{e}^{-\alpha(\lambda)x}\alpha(\lambda)P(x)\mathrm{dx} \tag{2.3}$$

where b is the depth of the detector and $\alpha(\lambda)$ is the spectrally dependent absorption coefficient. The absorption coefficient can be found from the complex refractive index of silicon. In these calculations one must include the reflectance, R, of the back of the detector. For the reflected photons the recombination probability used in the calculations is d_r, since reflected

photos that travel beyond the bulk region is considered negligible. The result of the integration is the following expression for the internal quantum deficiency[6]

$$\begin{aligned}\delta(\lambda, d_f, T, D, d_r, R, b) = &\frac{d_f}{T\alpha(\lambda)}(\mathrm{e}^{-T\alpha(\lambda)} + T\alpha(\lambda) - 1) \\ &- \frac{d_r}{(D-T)\alpha(\lambda)}\left((D\alpha(\lambda) - T\alpha(\lambda) + 1)\mathrm{e}^{-\alpha(\lambda)D} - \mathrm{e}^{-\alpha(\lambda)T}\right) \\ &+ d_r(\mathrm{e}^{-\alpha(\lambda)D} - \mathrm{e}^{-\alpha(\lambda)b}) \\ &+ (1 - R + R \cdot d_r)\mathrm{e}^{-\alpha(\lambda)b}\end{aligned} \tag{2.4}$$

The parameters in equation 2.4 has to be determined. This is achieved by fitting the deficiency function to the relative response of the trap detector. Since the parameters correspond to physical properties of the detector there are natural limitations in the fitting procedure. For instance can non of the parameters be less than zero. Some of the parameters can also be determined by other methods, for instance parts of the self-calibration procedure, leaving less parameters to be fitted.

The relative spectral response is found by comparing the responsivity of the detector to the responsivity of a spectrally flat detector. The model of the recombination probability has the property that for one particular depth the probability of recombination is zero, see figure 2.2. This is used to scale the relative responsivity of the detector.

Determining quantum deficiency parameters

To fit the parameters given in equation 2.4 a column vector $\mathbf{a}$, that has the parameters as elements, is introduced.

$$\mathbf{a} = \begin{pmatrix} a_1 \\ a_2 \\ a_3 \\ a_4 \\ a_5 \\ a_6 \\ a_7 \end{pmatrix} = \begin{pmatrix} k \\ d_f \\ T \\ D \\ d_r \\ R \\ b \end{pmatrix} \tag{2.5}$$

The first parameter in $\mathbf{a}$ is the factor which scales the relative response, while the other parameters are the parameters from equation 2.4. Measurements of the relative response of the detector, V, are made on n wavelengths λ. The wavelengths and response values can be written as two column vectors.

$$\boldsymbol{\lambda} = \begin{pmatrix} \lambda_1 \\ \lambda_2 \\ \vdots \\ \lambda_n \end{pmatrix} \qquad \mathbf{V} = \begin{pmatrix} V_1 \\ V_2 \\ \vdots \\ V_n \end{pmatrix} \tag{2.6}$$

A function $F(\lambda, \mathbf{a})$ is fitted to the measured relative response values by varying the elements in $\mathbf{a}$.

$$\mathbf{F(a)} = \begin{pmatrix} F(\lambda_1, \mathbf{a}) \\ F(\lambda_2, \mathbf{a}) \\ \vdots \\ F(\lambda_n, \mathbf{a}) \end{pmatrix} \tag{2.7}$$

Minimizing the generalized least-squares equation gives the function $F(\lambda, \mathbf{a})$ that best fit the measured relative response values[6].

$$\chi^2(\mathbf{a}) = \frac{1}{n-p}(\mathbf{V} - \mathbf{F(a)})^T \mathbf{u}^{(V)^{-1}}(\mathbf{V} - \mathbf{F(a)}) \tag{2.8}$$

where n is the number of measurement points, p is the number of parameters and $\mathbf{u}^{(V)}$ is the covariance matrix of the measured values at the different wavelengths λ_i. The measurements are independently made, so there will be no covariance in the measured values. $\mathbf{u}^{(V)}$ is therefore a diagonal matrix with elements $u_{ii}^{(V)} = \sigma_i^2$, where σ_i^2 is the variance of the response value V_i.

The fitted value of $\mathbf{a}$ is denoted $\hat{\mathbf{a}}$, and the estimated responsivity at wavelength λ is the scaled fit function

$$R(\lambda, \hat{\mathbf{a}}) = a_1 F(\lambda, \hat{\mathbf{a}}) \tag{2.9}$$

Uncertainty evaluation

In the case of two random variables x and y there will be a variance σ_x and σ_y for each variable and a covariance between the two variables $u(x, y)$. In the case of vector variables $\mathbf{x}$ and $\mathbf{y}$ there is a covariance matrix $\mathbf{u}(\mathbf{x}, \mathbf{y})$ where each matrix element $u_{m,n}(\mathbf{x}, \mathbf{y})$ is the covariance between the two random variables x_m and y_n[6].

The covariance in the responsivity estimate $\mathbf{R}(\lambda_i, \hat{\mathbf{a}})$ is expressed by

$$\mathbf{u}^{(\mathbf{R})} = \mathbf{r(a)}\mathbf{u}^{(\hat{\mathbf{a}})}\mathbf{r(a)}^T \tag{2.10}$$

where the matrix $\mathbf{r}(\mathbf{a})$ has, as matrix elements, the sensitivity coefficients $r(\mathbf{a})_{i\alpha} = \frac{\partial R(\lambda_i,\mathbf{a})}{\partial a_\alpha}$ of the responsivity $R(\lambda_i, \mathbf{a})$, and $\mathbf{u}^{(\hat{\mathbf{a}})}$ is the covariance matrix for the fitted parameters[6].

$\mathbf{u}^{(\mathbf{F})}$ is the covariance matrix for the fit function values $\mathbf{F}(\lambda_i, \hat{\mathbf{a}})$ given by

$$\mathbf{u}^{(\mathbf{F})} = \mathbf{f}(\mathbf{a})\mathbf{u}^{(\hat{\mathbf{a}})}\mathbf{f}(\mathbf{a})^T \tag{2.11}$$

where the matrix $\mathbf{f}(\mathbf{a})$ has as elements the sensitivity coefficients $f(\mathbf{a})_{i\alpha} = \frac{\partial F(\lambda_i,\mathbf{a})}{\partial a_\alpha}$.

Given the assumption that the fit $\hat{\mathbf{a}}$ is close to the true value of $\mathbf{a}$, so that $\mathbf{F}(\lambda_i, \mathbf{a})$ depends linearly on $\mathbf{a}$ near $\hat{\mathbf{a}}$, $\mathbf{u}^{(\hat{\mathbf{a}})}$ can be calculated form the covariance matrix of the sample values

$$\mathbf{u}^{(\hat{\mathbf{a}})} = [\mathbf{f}(\mathbf{a})^T\mathbf{u}^{(\mathbf{V})^{-1}}\mathbf{f}(\mathbf{a})]^{-1} \tag{2.12}$$

The calculations of the covariance of the responsivity values are given in matrix form as[6]

$$u(R_m, R_n) = \frac{\partial R_m}{\partial a_\alpha} \cdot u(a_\alpha, a_\beta) \cdot \frac{\partial R_n}{\partial a_\beta} = \frac{\partial R_m}{\partial a_\alpha} \cdot \frac{\partial a_\alpha}{\partial V_i} \cdot u(V_i, V_j) \cdot \frac{\partial a_\beta}{\partial V_j} \cdot \frac{\partial R_n}{\partial a_\beta} \tag{2.13}$$

where sum over equal indices is applied. Greek indices are used to identify the index of the fitting parameters in $\mathbf{a}$. The roman indices represents wavelength. The covariance matrix of the observed measurement noise $u(V_i, V_j) = 0$ unless $i = j$ with the variance of the individual measurements as its diagonal elements.

The uncertainty at each wavelength in the responsivity and the fit function is given as the square root of the diagonal elements of $\mathbf{u}^{(\mathbf{R})}$ and $\mathbf{u}^{(\mathbf{F})}$.

The correlation matrix for the responsivity is calculated by dividing the covariance of two responsivity values with the uncertainty of both values[6]

$$C(R_i, R_j) = \frac{u(R_i, R_j)}{u(R_i)u(R_j)} \tag{2.14}$$

The same procedure can be used to find the correlation matrix of the fit function.

2.2.3 The self-calibration procedure

The self-calibration procedure for photodetectors was developed by Zalewski and Geist in 1980[5]. This procedure determines the internal quantum deficiency of the diode by applying a bias voltage in appropriate regions of the diode. Since the internal quantum deficiency is determined without the use of a reference detector the method is known as the "self-calibration method".

To determine recombination losses to the rear of the junction a reverse bias voltage over the diode is applied. This voltage will increase the depletion width to the rear of the device, and thereby increase the responsivity since recombination of carriers created in the depletion region is highly unlikely. By monitoring the response of the detector, one can increase the applied voltage until the depletion region extend to a depth beyond which negligible radiation penetrates, and the quantum efficiency will saturate. The recombination losses to the rear of the junction is then known.

To determine the recombination losses at the silicon dioxide interface, a negative bias is applied over the oxide. This causes a negative charge to build up at the front surface, which counteracts the effect of the positive surface charge[5]. Increasing the applied bias will reduce the minority carrier concentration at the interface until the response saturates. The recombination losses caused by the surface charges is then known.

The problem with the self-calibration procedure is that it somehow alters the qualities of the detector. The responsivity of the detector is lower after the oxide bias have been applied[11]. The change in responsivity is most evident at lower wavelengths[7], which suggests that the alternation of the detector is in the front region of the detector.

2.3 Trap detectors

A trap detector consists of three photodiodes, arranged so that the reflection from each individual photodiode is directed onto a subsequent one[2]. To get the total photocurrent from the incident light, the current from the three detectors are summed. A schematic representation of a trap detector is given in figure 2.3.

The incident radiation undergoes five specular reflections before emerging from the trap detector, and is therefore almost totally absorbed. The reflectance of a trap detector is more than two magnitudes lower than the reflectance of a single silicon detector[2]. In a trap detector arrangement the first two detectors get irradiated at a 45° angle with opposite polarization, while the third detector gets irradiated at 0° and reflects the light directly back to the second detector. This reduces sensitivity to polarization of the

incident light[2], see figure 2.3.

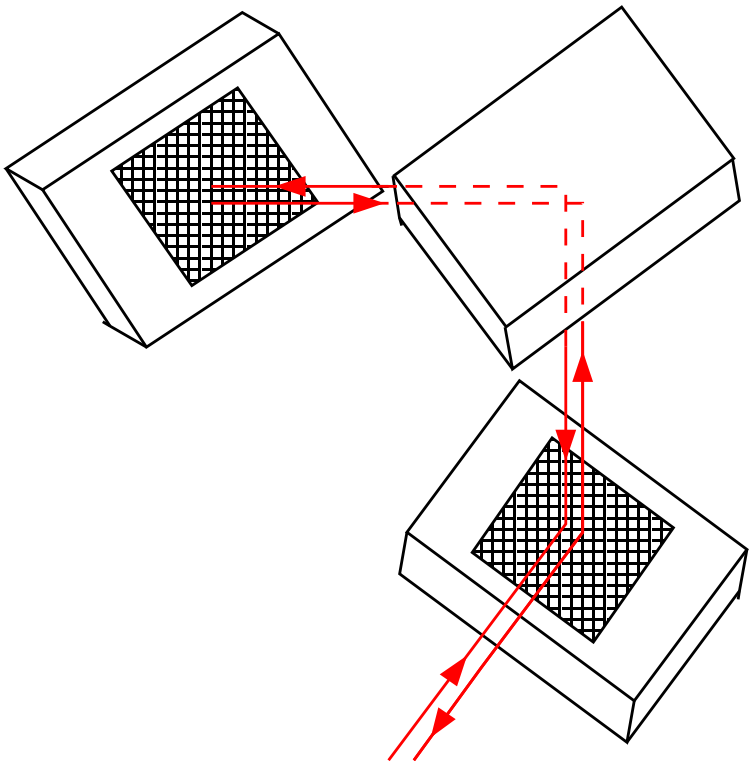

Figure 2.3: A schematic representation of the trap detector consisting of three photodiodes. The red line indicates the ray path of the incident light. The reflected ray is shifted slightly for illustrative purposes.

2.4 Pyroelectric detectors

A pyroelectric detector is a type of thermal detector, which means that the detector delivers a signal proportional to the increase in temperature caused by the incident electromagnetic radiation[12]. Pyroelectric detectors are made of materials with a permanent electrical polarization. The degree of this polarization is affected by temperature, and the surface charge of the material will therefore change when the temperature changes. Electrical contacts can carry some of this charge through an attached circuit, but the charge cannot flow in one direction indefinitely. Therefore the detectors can only measure changes in incident radiant flux[12]. Pyroelectric detectors are therefore suitable for measuring pulsed radiation. To measure a steady beam of incident light, a chopper has to be placed in the beam path to make the incident light vary at a constant frequency. It is important to keep the

chopping frequency stable, since pyroelectric detectors are very frequency sensitive[4]. The varying incident flux will produce a varying signal with amplitude proportional to the amplitude of the oscillating flux of the incident light[12].

Thermal detectors needs to absorb as much as possible of the incoming radiation to ensure a high sensitivity. This can be achieved by using a reflective hemisphere around the active element of the detector, and by applying a coating which has a high absorbance over the spectral region of interest[4]. By using a coating with absorbance that varies very slowly with wavelength, the detector will have a nearly flat spectral response. This is a huge advantage when calibrating thermal detectors. A disadvantage of thermal detectors is low sensitivities compared to other type of photodetectors. Pyroelectric detectors are also sensitive to mechanical vibration[12].

Chapter 3

Measurements

3.1 Determining the relative response of a silicon trap detector

A series of measurements at different wavelengths is necessary to determine the relative response of a silicon detector. The silicon detector with unknown response was a silicon trap detector of Hamamatsu diodes assembled by National Physical Laboratory (NPL). A cavity pyroelectric detector with a spectrally flat response, also assembled by NPL, was used as the reference in the measurements. The pyroelectric detector had a black coated activ element surrounded by a reflective hemisphere. Both the trap detector and the pyroelectric detector used in the measurements can be seen in figure 3.1. In addition to these detectors, another trap detector was needed to measure the spectrally dependent reflectance from the silicon trap detector.

The set-up used to measure the relative spectral response is shown in figure 3.2. A tunable laser was used as light source. The trap detector and the pyroelectric detector was attached to a "xy-instrument", so that the detectors could be moved up, down and sideways in a controlled manner. This made it possible to go back and forth between the two positions where the laser beam was directed into the trap detector, and where it was directed onto the pyroelectric detector. The ray was controlled by a laser power controller, which controls and monitors the laser output. Mirrors and a lenses were used to turn and focus the laser beam. Apertures also had to be used to eliminate scattered light. A computer controlled chopper was mounted so that it could be moved out of the beam path when measurements were done with the trap detector, and into the beam path when measurements were done with the pyroelectric detector. The chopper was frequency locked to 70 Hz, which prevents added uncertainty caused by the frequency dependence in the pyroelectric detector measurements.

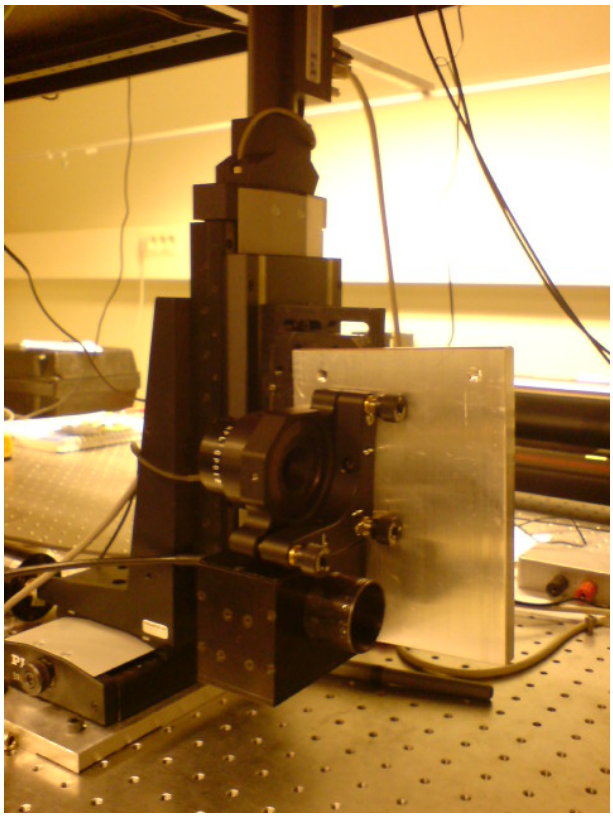

Figure 3.1: The silicon trap detector and pyroelectric detector attached to the "xy-instrument". The pyroelectric detector is placed above the trap detector.

The aim of these measurements was to see if the already promising results obtained, using the relative response procedure in a monochromator set-up[6], could be improved by using a laser as the light source.

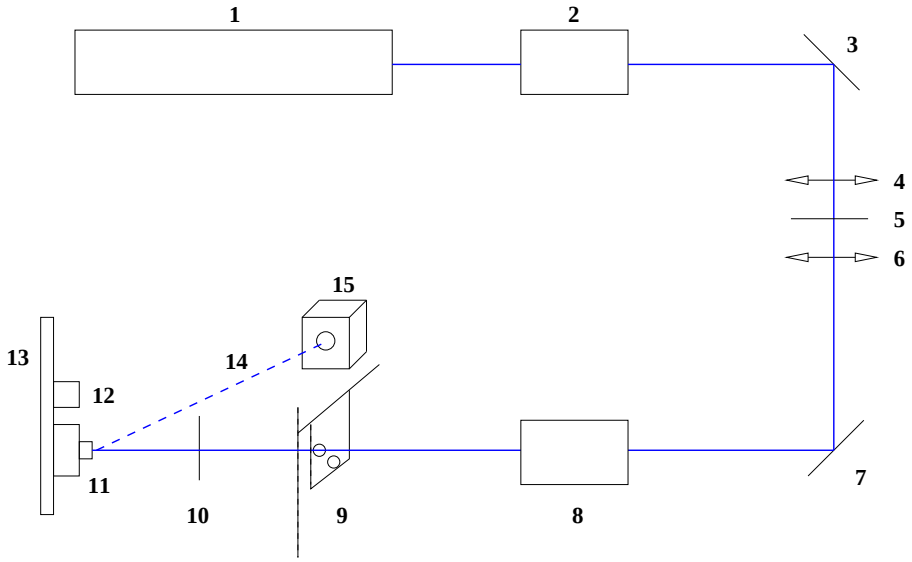

Figure 3.2: Set-up used for measuring the relative spectral response of the silicon detector. Laser beam is drawn to indicate ray path. 1) Laser, 2) Controller, 3) Mirror, 4) Lens, 5) Pin hole, 6) Lens, 7) Mirror, 8) Ray monitor, 9) Chopper, 10) Aperture, 11) Silicon trap detector, 12) Pyroelectric detector, 13) xy-instrument, 14) reflected beam, 15) Trap detector which measures the reflected beam.

3.2 The self-calibration procedure

As described in section 2.2.3, the self-calibration procedure changes the qualities of the silicon detector. The degradation is mainly in the front region of the detector, and is induced by the applied oxide bias[7]. If a response change at a lower applied voltage than the saturation voltage could be used to determine the recombination losses at the oxide interface, the degradation could possibly be kept at a negligible level.

In previous work[7] detectors which were partially covered with gold was used in self-calibration experiments. The gold-covered part was used to carry out the self-calibration procedure, since the gold layer could be used to apply a negative bias over the detector oxide. This allows the uncovered part of the detector to be used later in measurements when the responsivity of the detector is determined[7]. The uncovered part could also serve as a reference during the experiments. With this design there was no way of removing the gold from the surface after the experiments had been carried out, which is not a good permanent solution.

Figure 3.3: The gold covered glass plate which was used as an electrode to apply negative bias over the detector oxide. The gold layer is about 20 nm thick and is therefore transparent.

The aim of these measurements was to investigate whether it is possible to use a "removable gold film" to carry out the self-calibration procedure. This would make it possible to perform oxide bias experiments on detectors, then examine the degradation of the detector, and reuse the gold film on other detectors. If the front recombination losses could be determined without applying too high voltages, the "removable gold film" could be used to calibrate detectors without significantly degrading the detector or leaving permanent marks.

The "removable gold film" used in the experiments consists of a gold covered glass plate, with wires connected to the layer of gold at each side of the glass plate, see figure 3.3. This was used as the electrode to apply the oxide bias.

The electrode was fastened to the detector surface by placing it under a glass plate that was fastened to the same plate as the detector by two screws, see figure 3.4. As seen from the figure there are clearly visible "Newtons rings", which indicates that the electrode is shaped as a convex lens placed on the plane detector surface. There is therefore a layer of air of varying thickness between the electrode and the detector. The measurements could still be carried out by focusing the laser beam to the centre of the rings, assuming there is contact between the electrode and the detector at this point.

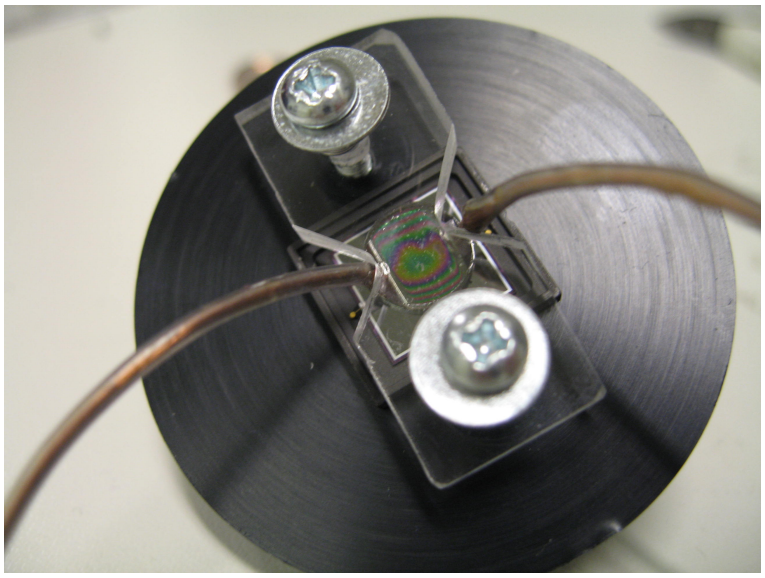

Figure 3.4: The single silicon detector used in the self-calibration experiments. The electrode is fastened to the detector surface using a glass plate fastened to the same plate as the detector. The interference rings, "Newtons rings", indicates that the electrode is shaped as a convex lens placed on the plane detector surface.

The single silicon detector with the electrode were mounted in a similar set-

up as used in the relative measurements, see figure 3.2. The chopper was removed since this was no longer needed, and the single silicon detector was placed in the laser beam. The reflectance was now measured by another single detector, instead of a trap detector, since the multiple reflections from the different layers covering the detector made it difficult to direct the reflection into a trap detector. As in the relative response measurements, the detector was mounted on the "xy-instrument", see figure 3.5, so that measurements could be done over the entire detector surface covered by the electrode. Measurements were done with -10 V applied oxide bias and without applied bias for reference. These measurements give information about how much influence the layer of air between the electrode and the detector has on the responsivity change with applied oxide bias. It also gives some information on whether the centre of the interference rings is suitable for self-calibration measurements.

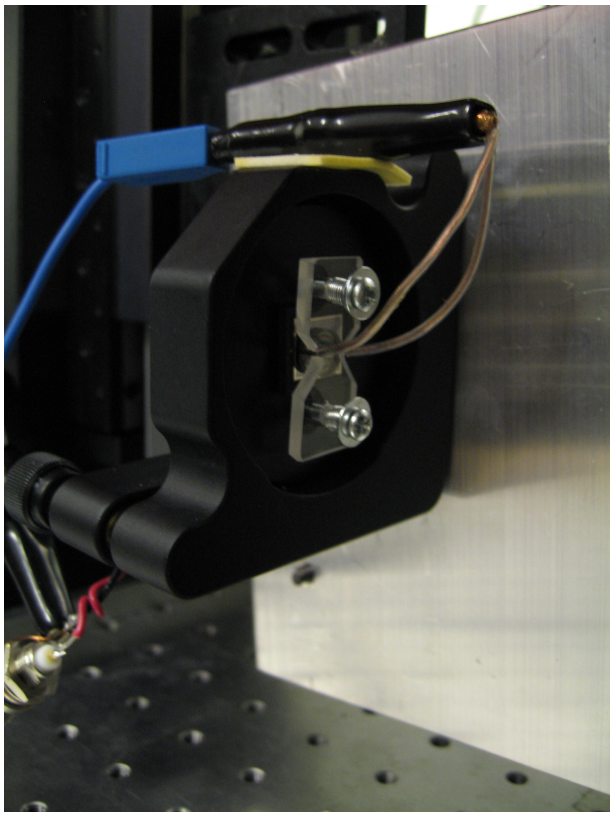

Figure 3.5: The single silicon detector with the gold electrode, used in the self-calibration experiments, mounted on the "xy-instrument".

The results from these measurements were initially hard to make sense of. Both the reflection and the light absorbed by the detector showed a similar

pattern of maximas and minimas, see section 5.2. It was expected that at the point where the reflection was minimal, the transmitted light into the detector would be maximal. The results could be influenced by the glass plate covering the electrode, or that the downward pressure on the electrode was applied from the screws on each side, which could cause the thickness of the air layer to vary differently from what was assumed. Therefore an alternative mounting of the electrode was tested, see figure 3.6. Holes were made in the glass plate for the contact points of the electrode, in an effort to make the pressure of the glass plate more directly downwards. It is, however, clear that there is still an uneven layer of air between the electrode and the detector which causes interference patterns, see figure 3.6. A hole was also made in the glass plate over the electrode, so that the laser beam could be directed onto the electrode without having to pass through the glass plate.

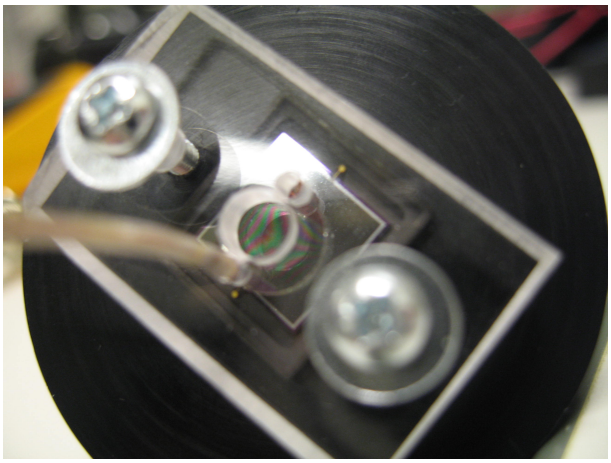

Figure 3.6: The single silicon detector with the electrode fixed to the surface in an alternative manner compared to the original mounting, see figure 3.4 A different interference pattern is visible here. There is a hole in the glass plate over the electrode which the laser beam can be directed into.

Chapter 4

Calculations

4.1 The relative response procedure

The calculations needed to determine the detector responsivity from the relative response measurements, and the uncertainty of the responsivity values, were performed using two Mathcad scripts written by *J. Gran*. One of the scripts fitted the values of equation 2.4 to the measured relative response following the procedure described in section 2.2.2.

The other script calculated the covariance matrices of the fit function values and the responsivity values. From these matrices the uncertainty, as well as the the correlation matrices, of the fit function values and the responsivity values was calculated. The calculations followed the procedure described in section 2.2.2.

4.2 The self-calibration procedure

Calculations of the reflectance and transmittance of the system shown in figure 3.6 were performed using the transfer matrix method in MATLAB. In this method the relationship between the magnitudes of the electric vectors on either side of the system is described as

$$\begin{pmatrix} E_1^+ \\ E_1^- \end{pmatrix} = \begin{pmatrix} P & Q \\ S & W \end{pmatrix} \begin{pmatrix} E_2^+ \\ E_2^- \end{pmatrix} \tag{4.1}$$

where E_1 is the magnitude of the electric field in the initial medium and E_2 is the magnitude in the final medium. The positive sign represents the transmitted wave and the negative sign represents the reflected wave. P, Q, S and W are the coefficients of the system matrix. This representation of the transfer matrix method is that used by *L. Ward* [13].

Table 4.1: The approximate values of the thickness of the layers in the system showed in figure 3.6, and refractive indices for each layer.

Material	Thickness	Refractive index
Air	*Initial medium*	1.0003
Glass	2 mm	1.5
Gold	20 nm	1.658 - 1.956i
MgF_2	70 nm	1.3899
SiO_2	30 nm	1.4701
Si	*Final medium*	5.5699 - 0.38795i

The system was assumed to consist of a stack of plane layers, where the incident medium was air, followed by a glass layer, a gold layer, a MgF_2 layer, a layer of air, and a SiO_2 layer. The final medium was silicon. The exact thickness of the different layers is unknown, so approximate values were used. The thickness of the layer of air vary with position, so the MATLAB script produced plots of the reflectance and transmittance as a function of the thickness of the air layer.

Values of the refractive indices was retrieved from `http://refractiveindex.info` using the closest available wavelength to 406.7 nm, which was the wavelength used in the experiments. The refractive index of glass was chosen to 1.5 as the exact composition of the glass used in the experiment is unknown, and therefore also the refractive index. The values used are given in table 4.1

In the calculations it was assumed that the laser beam was at normal incidence, which made the expressions of the reflectance and transmittance coefficients at each interface much simpler. The MATLAB script can be found in Appendix A.

Chapter 5

Results and Discussion

5.1 The relative response procedure

The measured reflectance from the trap detector was in good correspondence with the estimated reflectance, which can be seen in figure 5.1. The reflectance was only measured once for each available laser wavelength, so the measurement noise is unknown. However, the measured reflectance was so close to the estimated values that the measured result was considered accurate and was used in the calculations.

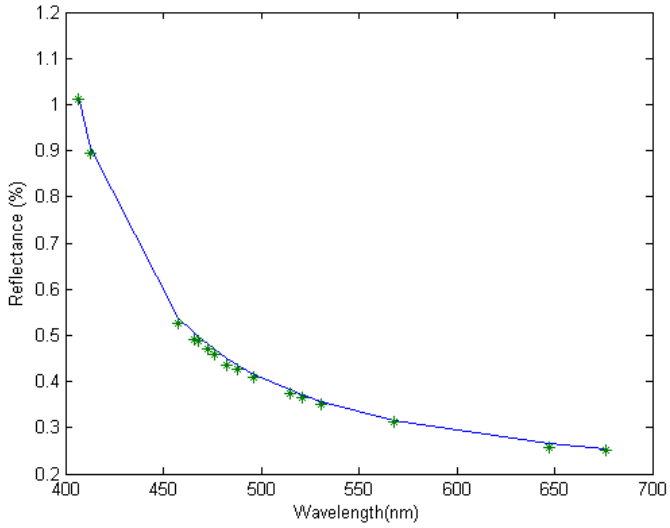

Figure 5.1: The green stars show the measured reflectance from the trap detector for the available laser wavelengths, the blue graph shows the simulated reflectance for a trap detector with 28 nm oxide thickness.

The expected quantum deficiency had a similar shape to the reflectance, but was lower for all wavelengths, see figure 5.2. The expected quantum deficiency was calculated using equation 2.4 and the values of k, d_f, T, D and d_r previously found by *J. Gran* and *A. S. Sudbø* [6] from fitting the relative response of a trap detector to equation 2.4. A guessed value, $b = 290$ nm, was used for the detector depth. The value of b will have a very small effect on the low wavelengths used in this experiment, so a deviation from the true value of b will not cause a large error. For the same reason the last term of equation 2.4 could be omitted, and an estimate of R was not needed.

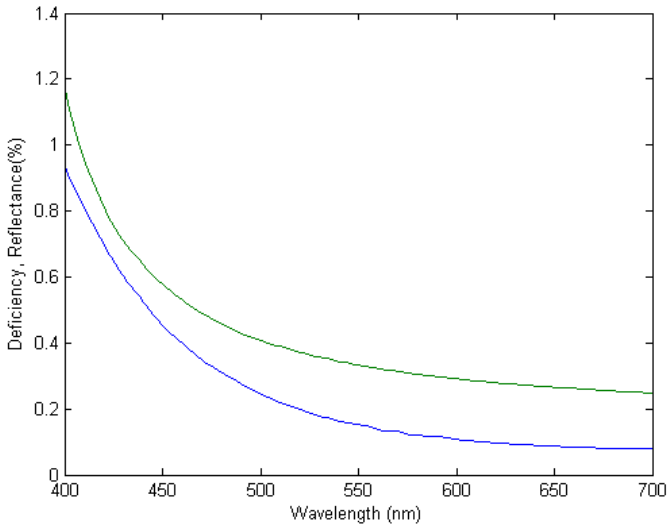

Figure 5.2: The blue graph shows the expected quantum deficiency, calculated from equation 2.4 omitting the last term and using the values for k, d_f, T, D and d_r found by *J. Gran* and *A. S. Sudbø* for a trap detector [6]. A detector depth $b = 290$ nm was chosen. The green graph shows the calculated reflectance.

The first attempt at measuring the relative response of the detector gave a quantum deficiency which had a very uneven and clearly faulty shape, see figure 5.3. The quantum deficiency is found using the relative response from the measurements and subtracting the reflectance and the ideal responsivity term. Since only the relative response is measured, the absolute value of the quantum deficiency cannot be estimated. Only the shape of the graph can be used to evaluate the success of the measurement.

Though the measurement noise is small, it is clear from figure 5.3 that there are errors in the measurements of similar magnitude to the deficiency. It was assumed that this error came from light scattered outside the opening in the hemisphere surrounding the pyroelectric detector. This will cause

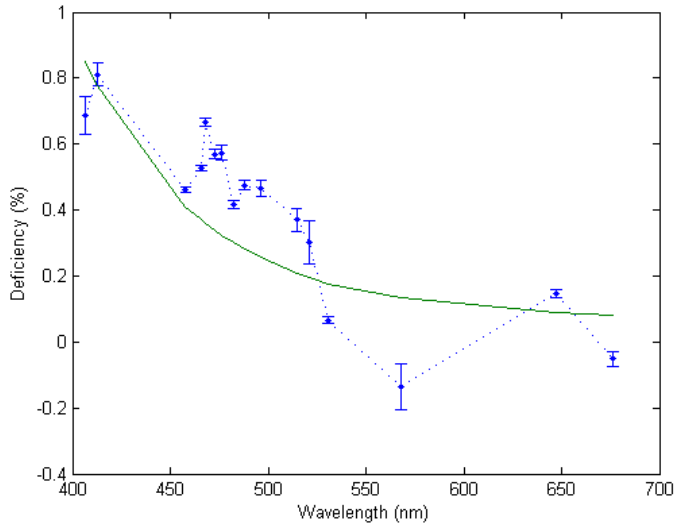

Figure 5.3: The blue dots is the quantum deficiency obtained from the first measurement of the relative response of the trap detector. The green graph is the expected quantum deficiency. It is clear that there is an error in the measurement larger than the measurement noise at the individual wavelengths.

a smaller amount of incident light onto the pyroelectric detector than the trap detector. Since the amount of scattered light varies with wavelength, the measured relative response also varies with wavelength. This causes the uneven shape of the quantum deficiency seen in figure 5.3.

Several attempts to focus the beam and eliminate scattered light failed. The only option remaining was to remove the reflective hemisphere of the pyroelectric detector, and direct the laser beam onto the active element of the detector, see figure 5.4. Though not visible in figure 5.4, the centre of the active element was damaged by the focused laser beam used in the experiments. This damaged spot could have a higher reflectivity than the rest of the detector surface, or in other ways influence the measurements.

Measurements with the hemisphere of the pyroelectric detector removed gave improved results, see figure 5.5. It is still clear that the shape of the quantum deficiency is not as smooth as desired. The results could probably be improved by adjusting for reflection from the surface of the pyroelectric detector. An attempt to measure this reflection was unsuccessful as it gave an even more faulty shape of the quantum deficiency. Fitting of the relative response of the trap detector to equation 2.4 had to be carried out without this correction

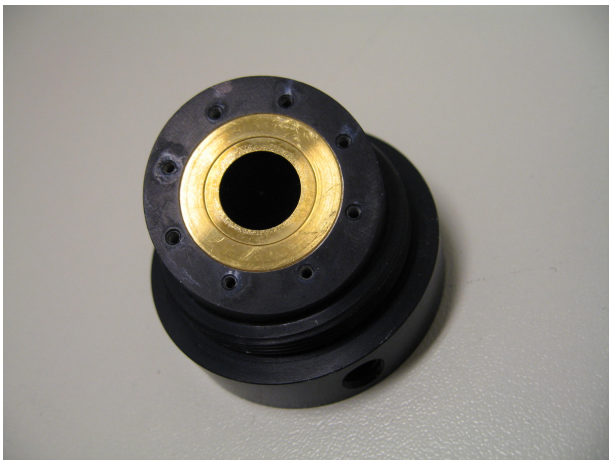

Figure 5.4: The pyroelectric detector with the reflective hemisphere removed.

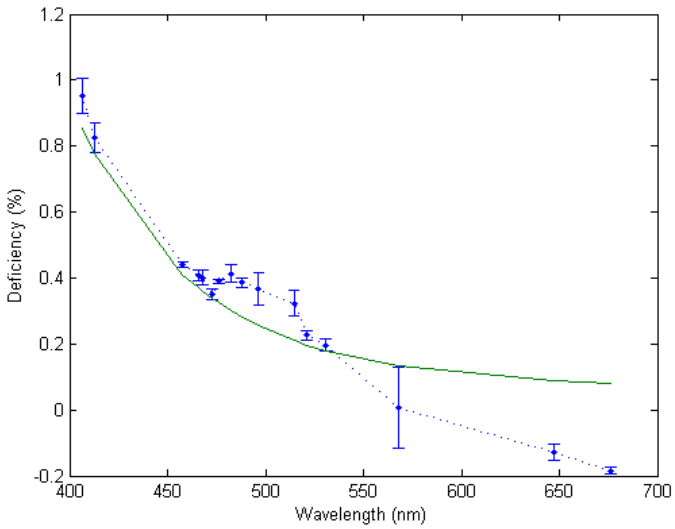

Figure 5.5: The blue dots are the quantum deficiency obtained from the final measurement of the relative response of the trap detector. The green graph is the expected quantum deficiency.

The final measurements of the relative response of the trap detector was run through the calculations which minimizes the expression in equation 2.8. The χ-value was over 100, which states that the fit was very pore. For comparison, the χ-value obtained by *J. Gran* and *A. Sudbø* in a similar experiment was 1.049[6]. The measurements at the three longest wavelengths were then excluded from the calculations, since they seem to deviate most

Table 5.1: The calculated parameters in the column vector **a** (2.5) from the relative spectral response.

k	0.34116
d_f	0.012897
T	0.43268 µm
D	35.618 µm
d_r	0.018165

from the expected value, see figure 5.5. Still the χ-value was as high as 48.524 for the best possible fit. The obtained parameters from the calculations are shown in table 5.1. The values of the detector depth, b, and the reflectance from the back side of the detector, R, was not fitted in the calculation since these will have little effect on the low wavelengths used in this experiment.

The obtained parameters in table 5.1 are not correct when compared to the results of similar experiment[6]. This is not unexpected considering that the best possible fit gave such a high χ-value. Particularly the scaling constant, k, and the values for D and d_r, deviates from previous results. The large deviation in D and d_r probably comes from the fact that only short wavelengths was used in the fitting procedure, and the values of D and d_r will have little influence at these wavelengths. The obtained value of d_r is larger than d_f, which is a clearly faulty result. In reality the recombination probability in the back region of the diode is much smaller than the recombination probability in the front region, since the back region of the diode is largely uniform material with low doping concentration and long lifetimes for the minority carriers. The front region has a much higher recombination probability, as explained in section 2.1.

In the calculations of the uncertainty and the correlation matrices of the responsivity and the fit function values, only the values for k, d_f and T was considered estimated. The values of D and d_f used in the calculation was taken from previous estimations by *J. Gran* and *A. S. Sudbø*[6] and considered to be exact. The values used in the calculations was $D = 16.08$ µm and $d_r = 1.176 * 10^3$. The chosen value of the detector depth $b = 290$ µm was still used.

The relative uncertainty of the responsivity and the fit function values can be seen in figure 5.6. These results cannot be considered accurate since one of the assumptions in the calculations was that the estimated value of **a** was close to the true value. The large χ-value from the minimization of equation 2.8 clearly shows that this is not the case.

The estimated correlation matrices for the fit function and the responsivity values can be seen in figure 5.7 and 5.8. These show the same characteristics as in earlier experiments[6]. The correlation matrix of the fit function values

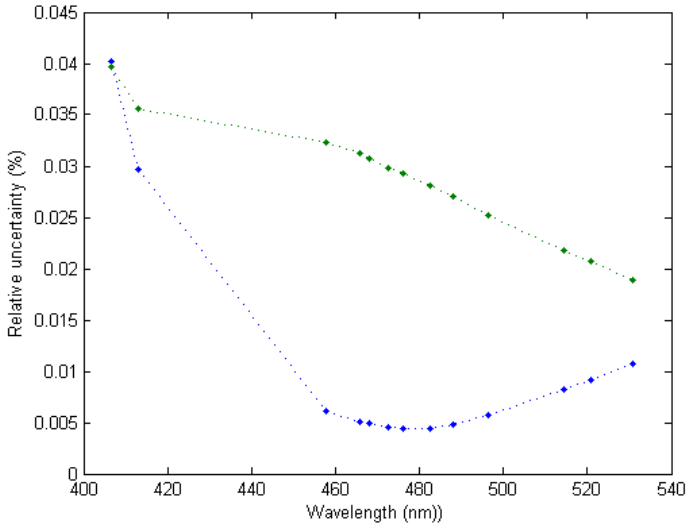

Figure 5.6: The green dots show the relative uncertainty of the responsivity values. The blue dots show the relative uncertainty of the fit function values.

shows a diagonal shape, while the correlation matrix of the responsivity values has a flat shape, caused by the uncertainty in the scaling constant.

The relative response procedure gave initially very promising results. A "hybrid self-calibration procedure", which combines the relative response procedure with parts of the self-calibration procedure, gave results with an accuracy close to that obtained by cryogenic radiometers[6]. This could be further improved using a laser as the light source, but to avoid damaging the active element of the pyroelectric detector it would probably be necessary to remove the reflective hemisphere of the detector and use a less focused laser beam. In this case the reflectance of the active element must be determined and adjusted for in the calculations.

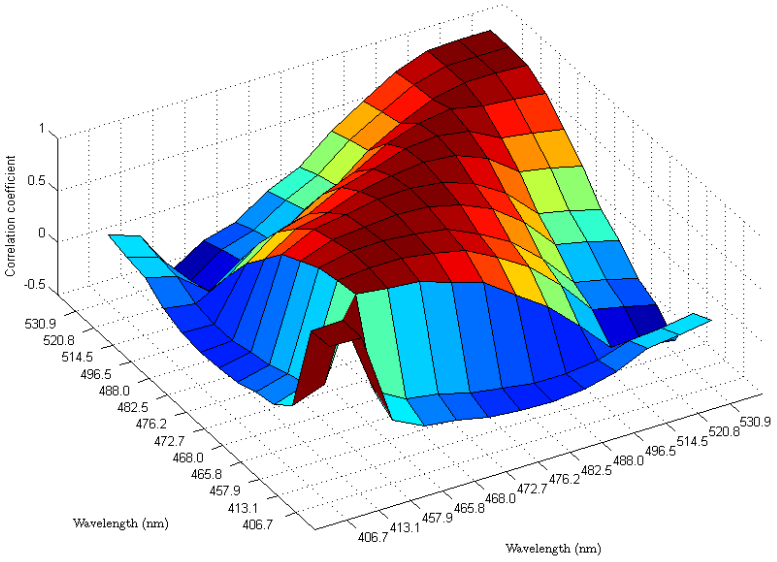

Figure 5.7: The correlation matrix for the fit function values.

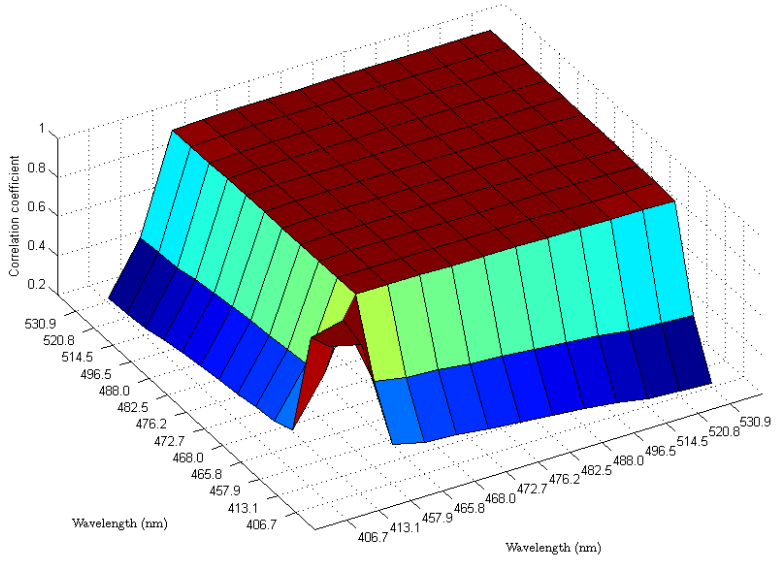

Figure 5.8: The correlation matrix for the responsivity values.

5.2 The self-calibration procedure

Measurements performed on the detector covered by the electrode, as shown in figure 3.4, gave some unexpected results, see figure 5.9. The reflectance was as expected, see figure 5.10. It is cancelled out in a ring shaped pattern by destructive interference, as could be seen before the measurements started, see figure 5.9 The measured response of the detector, however, was not as initially expected. The response of the detector was low at the centre of the electrode, and peaked in a ring shaped pattern similar to the pattern of the reflection. One would expect the detector response to be largest when a minimal amount of the light is reflected, and get smaller as the reflectance increases. In that case, the sum of the reflected light and the light absorbed by the detector would be uniform when plotted as a function of position. Instead the sum gives an even more evident ring pattern, since the response and reflectance vary in a similar manner.

The change with an applied oxide bias of -10 V also gave the same pattern both for the detector and the reflection, see figure 5.9 and 5.10. The ring shaped change in the reflection can be explained by the increased number of electrons at the detector surface when a negative bias is applied. This would give the detector surface more metallic qualities, which would increase the reflection from the surface when the reflection is not cancelled out by destructive interference. The change in response from the detector is somewhat harder to explain. It was expected that the increase in response would be largest at the centre where the contact between the electrode and the detector surface is best. But there is only a small positive change at the centre, see figure 5.9. And the ring shaped pattern is still visible around the centre.

The measurements performed on the detector with the electrode mounted as seen in figure 3.6 gave similar results. The measured reflection, see figure 5.12, gave as expected the same interference pattern as seen in figure 3.6. The response of the detector also gave a pattern similar to the interference pattern, see figure 5.11. The peaks and valleys in the pattern do not correspond completely with the ones in the reflection pattern, but the sum of the absorbed and reflected light is far from uniform.

The change with an applied oxide bias of -10 V was as expected for the reflection, see figure 5.12. The change is largest for the interference peaks. This is the same result as obtained in the first measurements. The detector gave very little change in response with applied oxide bias, see figure 5.11. The change is slightly positive, though this is not apparent from the figure, which is as expected. The interference pattern is, as in the first measurements, still visible.

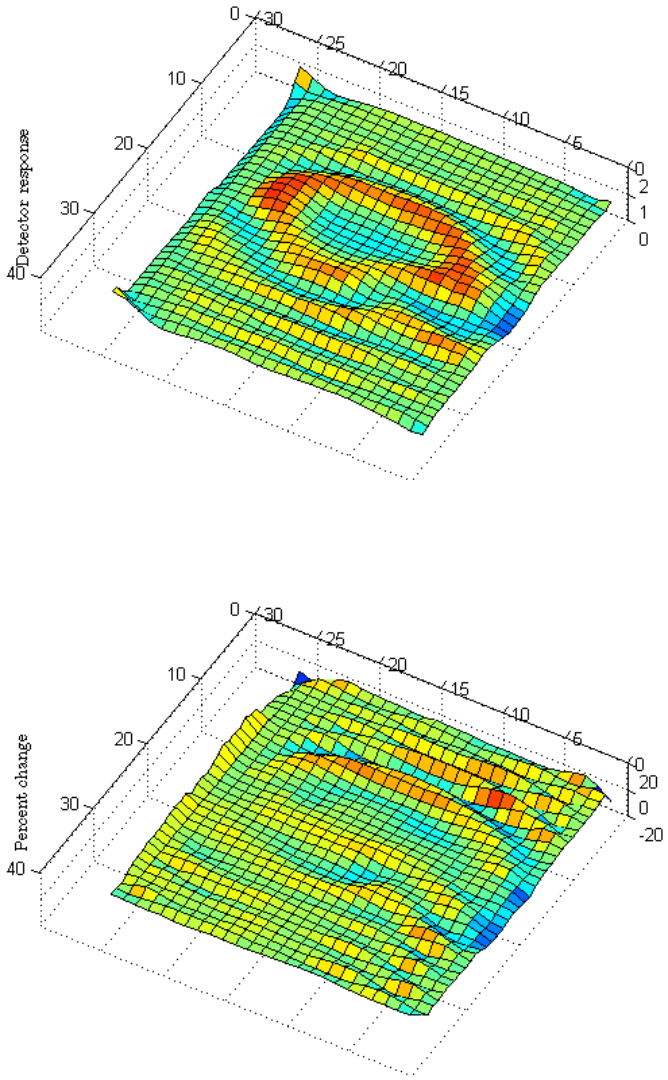

Figure 5.9: The top figure shows the response of the detector covered with the electrode as shown in figure 3.4. The bottom figure shows the responsivity change, expressed in percentage, with applied oxide bias of -10 V. Each square is a measurement point, and the total length and width of the measurement area is 5 mm and 7 mm.

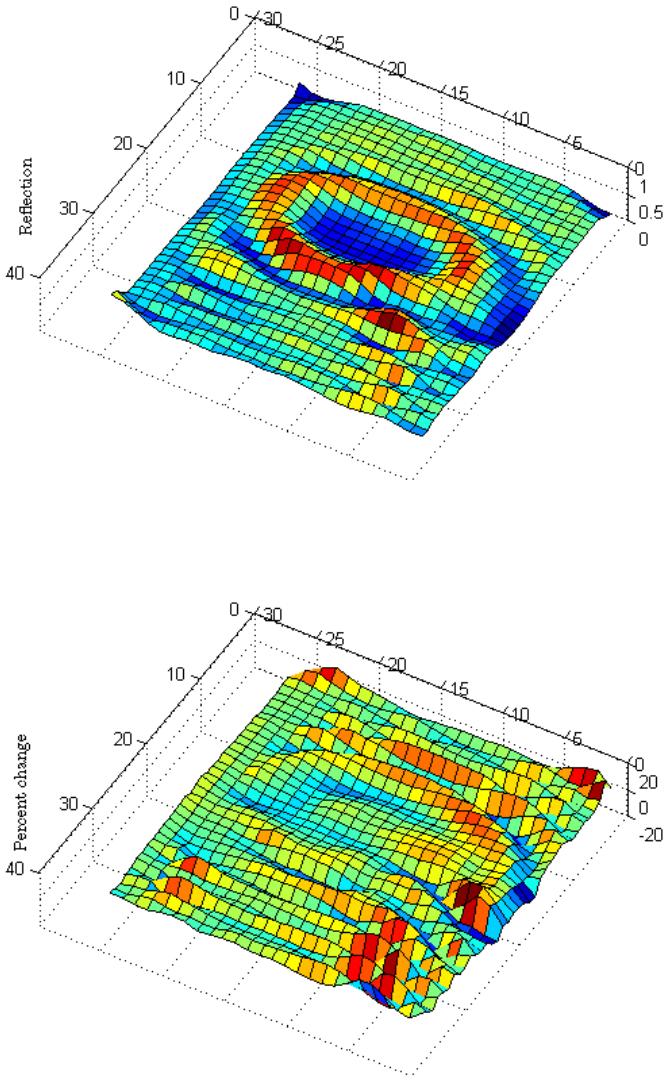

Figure 5.10: The top figure shows the measured reflection from the detector surface covered with the electrode as shown in figure 3.4. The bottom figure shows the change in reflection, expressed in percentage, with applied oxide bias of -10 V. Each square is a measurement point, and the total length and width of the measurement area is 5 mm and 7 mm.

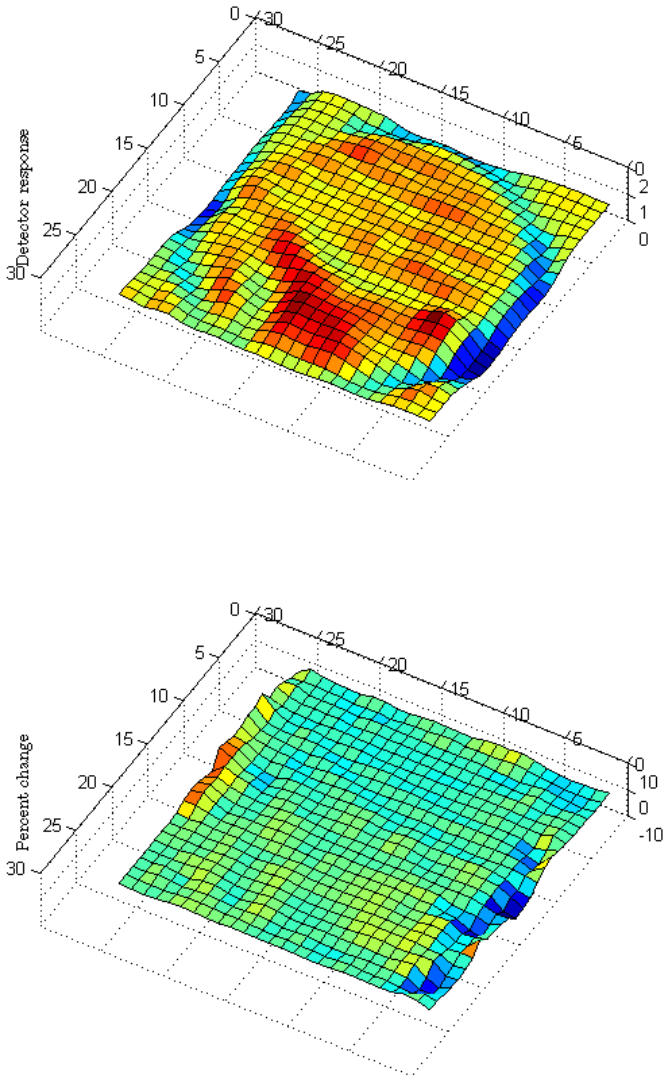

Figure 5.11: The top figure shows the measured response of the detector with the electrode mounted as shown in figure 3.6. The bottom figure shows the change in response, expressed as percentage, with an applied oxide bias of -10 V. Each square is a measurement point, and both the length and the width of the measurement area is 5 mm.

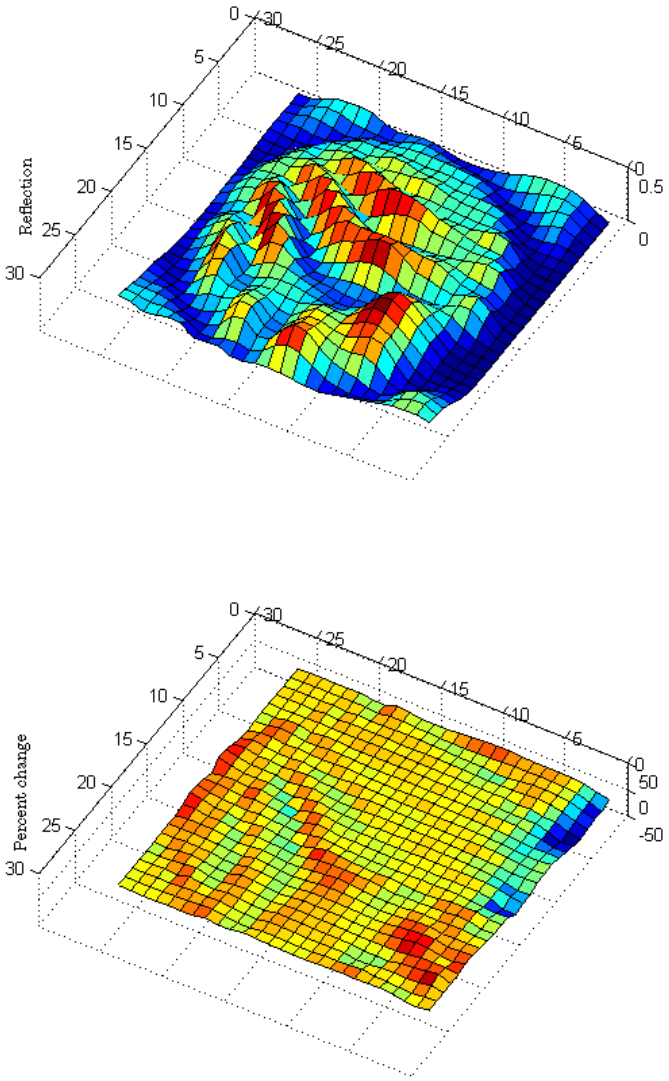

Figure 5.12: The top figure shows the measured reflection from the detector surface covered with the electrode mounted as shown in figure 3.6. The bottom figure shows the change in reflection, expressed in percentage, with an applied oxide bias of -10 V. Each square is a measurement point, and both the length and the width of the measurement area is 5 mm.

The fact that the transmitted light into the silicon and the reflected light did not give a uniform value over the surface, indicates that some of the light is absorbed in the gold layer. If no light was absorbed, the reflectance should peak when the transmittance is minimal. Calculations using the transfer matrix method, as described in section 4.2, showed that with the set-up used in these measurements, both the transmittance and the reflectance is low when the layer of air has zero thickness, see figure 5.13 and 5.14. The reflectance and transmittance give a wavelike pattern as the thickness of the air layer increases. The peaks and valleys does not completely coincide, but the sum of the reflectance and transmittance still give a clearly visible wave pattern, see figure 5.15 This is not the case if absorption in the gold layer is not included. Calculations, using a thickness of the gold layer equal to zero, gave a transmittance and reflectance that summed to unity.

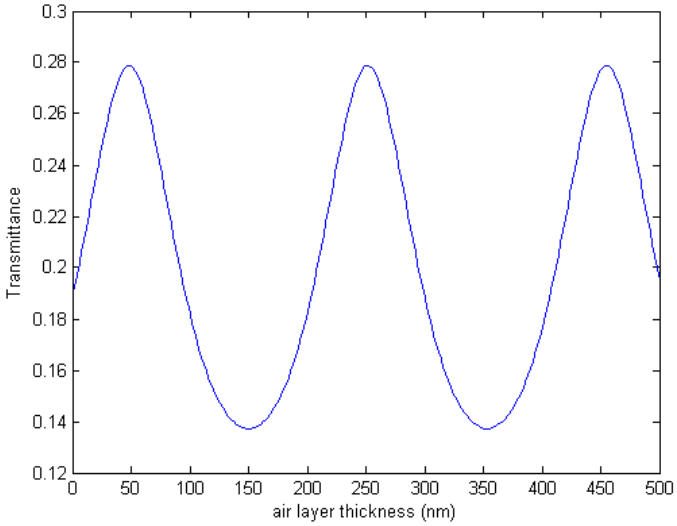

Figure 5.13: The calculated transmittance from the system shown in figure 3.6 as a function of thickness of the air layer between the electrode and the detector.

The simulation can only qualitatively explain the measurement results. Since the thickness of the different layers are not exactly known, nor the variations in the thickness of the layer of air, the simulations cannot predict the measurement results, only be used to explain some of its properties.

The calculations does, however, show that absorption in the gold layer cannot be ignored. This absorption severely affects the measurements, even with a thickness as small as 1/20 of the wavelength. The electric field strength in gold will influence the absorption, and this weighs against using a gold film in self-calibration experiments, as this introduces another source of error. The

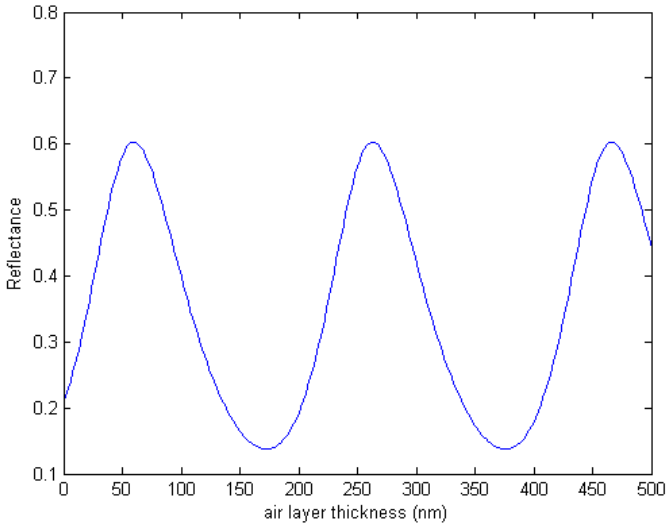

Figure 5.14: The calculated reflectance from the system shown in figure 3.6 as a function of thickness of the air layer between the electrode and the detector.

fact that an applied voltage changes the reflectance can also be a problem.

The change in response with applied oxide bias does, despite the difficulties encountered in this experiment, behave somewhat as expected, see figure 5.16. With applied bias the responsivity increases, though in a more uneven manner than in previous oxide bias experiments[7]. The responsivity change seem to saturate at 1.7%, before it increases further when the applied voltage exceeds 18 V. This suggests that the applied voltage became to high and that the oxide punctured. However, the uncertainty in the measurements is too large to state this for certain. The reflectance also increased in these measurements, as the applied voltage increased, with almost 1% with an oxide bias of 20 V.

If such a gold electrode is to be used in the self-calibration procedure , it would be a strong advantage to have as completely plane a surface as possible to eliminate interference patterns. Or else a small change in position of the laser beam will influence the measurements tremendously, as the amount of transmitted light is not the same at a different position. It would also be an advantage to design the thickness of the different layers to optimise the amount transmitted light.

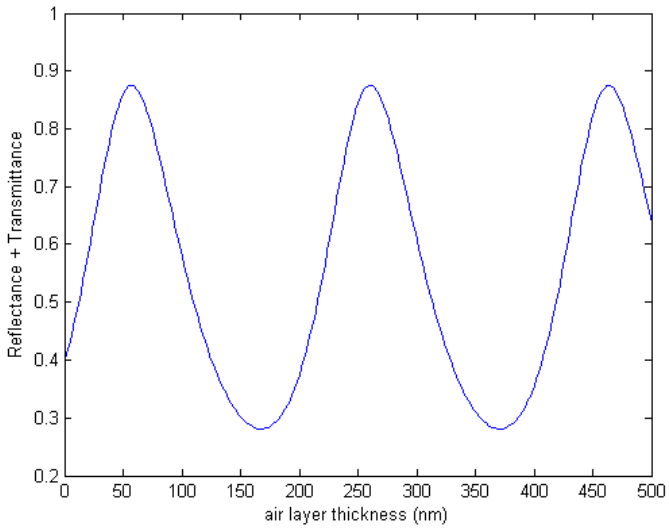

Figure 5.15: The sum of the calculated reflectance and transmittance from the system shown in figure 3.6 as a function of thickness of the air layer between the electrode and the detector. The amount of the incident light not reflected or transmitted is absorbed in the layer of gold.

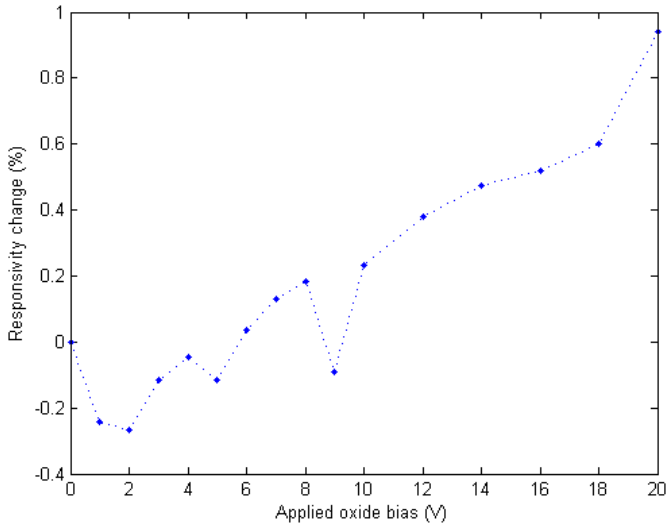

Figure 5.16: The change in responsivity of a silicon detector as a function of applied oxide bias, using the gold electrode.

Chapter 6

Conclusion

Silicon photodetectors meets many of the demands of an ideal detector, and can easily be used to carry out high accuracy measurements. Today silicon photodetectors have to be calibrated towards a cryogenic radiometer to best determine the detector responsivity. If silicon photodetectors are to be used as primary standards, the responsivity of the detector has to be determined independently.

The relative response procedure for determining the responsivity has in earlier experiments provided very promising results. The "hybrid self-calibration procedure", which combines the relative response procedure and parts of the self-calibration procedure has given results with an accuracy comparable to the accuracy of cryogenic radiometers. These measurements was obtained using a monochormator as the light source, and could be further improved by replacing the monochromator with a laser. When using a laser it is important to eliminate scattered light in the measurements, as this will introduce an extra spectrally dependent error. If a pyroelectric detector is used as the spectrally flat reference detector, it is important to avoid focusing the laser beam too much, as this can harm the detector and add uncertainty to the measurements. It might be necessary to use the pyroelectric detector without a reflective hemisphere to collect all the light of the less focused beam. In this case the spectrally dependent reflectance of the active element of the detector has to be determined.

The self-calibration procedure has some obstacles that need to be overcome before it can be used to determine the responsivity of photodetectors. It is necessary to investigate further how severe the degradation of the diode is after the oxide bias has been applied, and if there is ways to keep this degradation on a negligible level. The gold electrode investigated in this master's thesis will be useful in such experiments, as it can be used to apply the oxide bias on several detectors without leaving permanent marks. It is important that such a gold electrode is produced under controlled conditions,

making the surface as plane as possible to eliminate interference patterns in the measurements. It would also be an advantage to design the thickness of the different layers to optimise the amount of transmitted light.

References

[1] Qvision (Online). URL `http://www.qvision.no/default.asp?V_ITEM_ID=664`.

[2] N. P. Fox. Trap detectors and their properties. *Metrologia*, 28, 1991.

[3] Norwegian Metrology Service (Online). URL `http://www.justervesenet.no/Modules/theme.aspx?ObjectType=Article&ElementID=673&Category.ID=826`.

[4] National Physical Laboratory. Optical radiation detectors, a pratical course on measurement techniques and standards, 1993.

[5] E. F. Zalewski and J. Geist. Silicon photodiode absolute spectral response self-calibration. *Applied optics*, 19(2), April 1980.

[6] J. Gran. *Accurate and independent spectral response scale based on silicon trap detectors and spectrally invariant detectors.* PhD thesis, University of Oslo, 2005.

[7] G. Flatøy. *Using Silicon Photodiodes as Primary Standards for Optical Power Measurements.* NTNU, December 2008.

[8] B. G. Streetman and S. K. Banerjee. *Solid State Electronic Devices.* Pearson Prentice Hall, 6th edition, 2006.

[9] E. F. Zalewski and C. R. Duda. Silicon photodiode device with 100% external quantum efficiency. *Applied optics*, 22(18), September 1983.

[10] T. R. Gentile, J. M. Houston, and C. L. Cromer. Realization of a scale of absolute spectral response using the national institute of standards and technology high-accuracy cryogenic radiometer. *Applied optics*, 35 (22), August 1996.

[11] J. Verdebout and R.L. Booker. Degradation of native oxide passivated silicon photodiodes by repeted oxide bias. *Journal of applied physics*, 55(2), January 1984.

[12] R. McCluney. *Introduction to Radiometry and Photometry.* Artech House, 1994.

[13] L. Ward. *The Optical Constants of Bulk Materials and Films.* Institute of Physics Publishing, 2nd edition, 1994.

Appendix A

MATLAB script to calculate reflectance and transmittance

The system is as follows: Air | Glass | Gold | MgF_2 | Air | SiO_2 | Silicon

The script produces plots of the transmittance and reflectance of the system as a function of the thickness of the layer of air.

```
%refractive indices from http://refractiveindex.info, using the
%closest available wavelength
k = 2*pi/(406.7*10^-9);
nAir = 1.00028276;
nGl = 1.5;
nAu = (1.658 - 1.956i);
nMF = 1.3899;
nSiO2 = 1.4701;
nSi = 5.569931 - 0.387951i;
%Wave number for the different materials
kAir = k*nAir;
kGl = k*nGl;
kAu = k*nAu;
kMF = k*nMF;
kSiO2 = k*nSiO2;
kSi = k*nSi;
%Thickness of the layers
dGl = 2*1^-3;
dAu = 20*10^-9;
dMF = 70*10^-9;
dSiO2 = 30*10^-9;
%reflectance and transmittance coefficients for light at normal
    incidence
%for each interface
t1 = (2*nAir)/(nAir + nGl);
r1 = (nAir - nGl)/(nAir + nGl);
t2 = (2*nGl)/(nGl + nAu);
r2 = (nGl - nAu)/(nGl + nAu);
t3 = (2*nAu)/(nAu + nMF);
r3 = (nAu - nMF)/(nAu + nMF);
```

```
t4 = (2*nMF)/(nMF + nAir);
r4 = (nMF - nAir)/(nMF + nAir);
t5 = (2*nAir)/(nAir + nSiO2);
r5 = (nAir - nSiO2)/(nAir + nSiO2);
t6 = (2*nSiO2)/(nSiO2 + nSi);
r6 = (nSiO2 - nSi)/(nSiO2 + nSi);
AirLayer = (0 : 2 : 500);
R = (0 : 2 : 500);
T = (0 : 2 : 500);
Total = (0 : 2 : 500);
for j = 0:250
d =j*2*10^-9;
M1 = [1/t1 r1/t1; r1/t1 1/t1];
M2 = [exp(1i*kGl*dGl) 0; 0 exp(-1i*kGl*dGl)];
M3 = [1/t2 r2/t2; r2/t2 1/t2];
M4 = [exp(1i*kAu*dAu) 0; 0 exp(-1i*kAu*dAu)];
M5 = [1/t3 r3/t3; r3/t3 1/t3];
M6 = [exp(1i*kMF*dMF) 0; 0 exp(-1i*kMF*dMF)];
M7 = [1/t4 r4/t4; r4/t4 1/t4];
M8 = [exp(1i*kAir*d) 0; 0 exp(-1i*kAir*d)];
M9 = [1/t5 r5/t5; r5/t5 1/t5];
M10 = [exp(1i*kSiO2*dSiO2) 0; 0 exp(-1i*kSiO2*dSiO2)];
M11 = [1/t6 r6/t6; r6/t6 1/t6];
MS = M1*M2*M3*M4*M5*M6*M7*M8*M9*M10*M11;
r = MS(2,1)/MS(1,1);
t = 1/MS(1,1);
R(j+1)= abs(r)^2;
T(j+1) =real(nSi)*(abs(t)^2)/nAir;
Total(j+1) =abs(r)^2 + real(nSi)*(abs(t)^2)/nAir;
end
plot(AirLayer, T), xlabel('air layer thickness (nm)'), ylabel('
    Transmittance');
%plot(AirLayer, R), xlabel('air layer thickness (nm)'), ylabel('
    Reflectance');
%plot(AirLayer, Total), xlabel('air layer thickness (nm)'), ylabel('
    Reflectance + Transmittance');
```